Liquid Crystals
Publication details, including instructions for authors and subscription information:
http://www.informaworld.com/smpp/title~content=t713926090

A mathematical model for blade coating of a nematic liquid crystal

J. Quintans Carou[a]; N. J. Mottram[a]; S. K. Wilson[a]; B. R. Duffy[a]
[a] Department of Mathematics, University of Strathclyde, Livingstone Tower, Glasgow, United Kingdom

To cite this Article Carou, J. Quintans , Mottram, N. J. , Wilson, S. K. and Duffy, B. R.(2007) 'A mathematical model for blade coating of a nematic liquid crystal', Liquid Crystals, 34: 5, 621 — 631
To link to this Article: DOI: 10.1080/13682820701261801
URL: http://dx.doi.org/10.1080/13682820701261801

Liquid Crystals, Vol. 34, No. 5, May 2007, 621–631

A mathematical model for blade coating of a nematic liquid crystal

J. QUINTANS CAROU, N.J. MOTTRAM*, S.K. WILSON and B.R. DUFFY

Department of Mathematics, University of Strathclyde, Livingstone Tower, 26 Richmond Street, Glasgow, G1 1XH, United Kingdom

(*Received 5 July 2006; in final form 15 December 2006; accepted 15 December 2006*)

The standard industrial process of blade-coating is now being used to produce new liquid crystal displays (LCDs) in which a liquid crystal and optical layers are coated onto a substrate. Motivated by this new LCD manufacturing process, we use the Ericksen–Leslie equations to develop a simple mathematical model for blade coating of a nematic liquid crystal. The direction and uniformity of the director are important factors for the performance of the displays, particularly when this alignment is 'frozen in' within optical layers. For this reason we investigate the flow and director within a liquid crystal film both after emerging from the region under a blade (the so-called 'drag-out' problem) and before entering the region under a blade (the so-called 'drag-in' problem). We restrict our attention to thin films and small director angles, and we study two particular cases in which either orientational elasticity effects or flow effects dominate the alignment of the liquid crystal. We find that there is a unique solution of the drag-out problem, whereas there may be multiple solutions of the drag-in problem. When orientational elasticity effects dominate we obtain a simple analytical solution for the director. When flow effects dominate we find that the director is uniform in the bulk of the liquid crystal, which exhibits thin orientational boundary layers near the substrate and the free surface, within which the director orientation changes rapidly from its prescribed boundary value to the flow alignment angle. These boundary layers may be potential locations for the nucleation of defects.

1. Introduction

Liquid crystal displays (LCDs) are used in a wide range of applications from flat-screen televisions and laptop computers to mobile telephones and pocket calculators because they are thin, light and have a low power consumption. LCD technology exploits a simple electro-optical effect and is now well understood. However, the constraints imposed by using glass substrates mean that standard manufacturing techniques cannot be used for novel applications in which the display needs to be curved or deformable. Moreover, the current manufacturing process of LCDs, involving batch processing of sheets of glass, means that only rectangular displays can be produced in a cost effective way [1]. At present the liquid crystal is usually introduced between the two glass substrates using capillary action and/or under an applied pressure difference. A 'one-drop-fill' method can also be used in which a prescribed amount of liquid crystal material is dropped onto one substrate and then a second substrate is overlaid under vacuum.

An alternative manufacturing process has been discussed for a number of years, but has only recently been implemented [2]. In this process the liquid crystal is coated onto a plastic substrate (usually treated with appropriate barrier layers to prevent the passage of water and oxygen) using a blade-coating technique. This coating technique is relatively standard in other areas of technology [3], but has only recently been used to produce LCDs. The liquid crystal material may also contain a small amount of polymer-inducing material which when cured (by means of UV light) will crosslink to form a polymer matrix. If, at the same time (i.e. while the polymerization process takes place) a phase separation occurs (aided by localized UV illumination), then the polymer matrix can form a second (upper) substrate which encapsulates the liquid crystal material to form the finished display. Optical layers such as polarizers and colour filters could also then be applied using the same method. In contrast to batch processing techniques which are hampered by the need to handle, process and transport large sheets of glass, this process has the considerable advantage that it can be performed by roll-to-roll printing, which will reduce manufacturing time, increase throughput, and thereby reduce manufacturing costs. There are at present a number of technological hurdles to overcome in order to utilize fully these roll-to-roll techniques (e.g. the ability to produce printable

*Corresponding author. Email: nigel.mottram@strath.ac.uk

Liquid Crystals
ISSN 0267-8292 print/ISSN 1366-5855 online © 2007 Taylor & Francis
http://www.tandf.co.uk/journals
DOI: 10.1080/13682820701261801

TFTs or organic electronics). However, the initial cost of setting up a roll-to-roll production facility for LCDs is estimated to be around $100 million, which is much less than a comparable (generation-7) LCD plant [1]. The main driver behind the interest in using roll-to-roll printing to manufacture LCDs may therefore be economic considerations, but developing this process will also enable the production of truly flexible displays which have been predicted for a number of years and could revolutionize the display industry. This new manufacturing process using roll-to-roll printing may also be used to produce other kinds of displays in the future, such as organic light emitting diodes, which are currently manufactured using glass substrates, but which are believed by many to be the 'natural' choice for a flexible display [1].

During the coating process the liquid crystal is usually deposited while it is in an isotropic phase, that is, when the orientational order of the liquid crystal is zero. However, coating in the isotropic phase may be difficult to achieve because substrates can induce a significant amount of ordering in the system, or may be disadvantageous compared with coating in the ordered phase. If an ordered phase is induced, either by the underlying substrate or by the blade coating process, then unwanted misalignment and possibly even defects may be induced in the system.

For these reasons, in this exploratory study we will consider the flow and alignment during blade-coating of a nematic liquid crystal onto a planar substrate. In previous work [4] we described the flow and alignment of a liquid crystal in the region under a blade; here we describe the flow and alignment of a liquid crystal film after emerging from the region under a blade (the so-called 'drag-out' problem) and before entering the region under a blade (the so-called 'drag-in' problem), as shown in figure 1. In this work we will use analytical and numerical techniques to analyse the Ericksen–Leslie equations [5–7] governing the fluid velocity and pressure and the director, in cases when both the aspect ratio of the film of liquid crystal and the director angle are small.

2. Governing equations

We consider a thin film of liquid crystal of constant density ρ and constant surface tension coefficient γ flowing with a free surface $z=h(x)$ on a horizontal planar substrate $z=0$. The substrate moves with constant velocity U (>0) in the positive x direction away from (or towards) a fixed blade with lower surface $z=b(x)$ which lies between $x=0$ and $x=L$ (see figure 1). When the substrate moves away from the blade [the so-called 'drag-out' problem shown in figure 1 (*a*)] we assume that there is a reservoir of liquid crystal of prescribed depth R upstream of the blade (i.e. in $x<0$), and when the substrate moves towards the blade [the so-called 'drag-in' problem shown in figure 1 (*b*)] we assume that there is a similar reservoir downstream of the blade (i.e. in $x>L$). Gravity acts in the negative z direction. We assume that a steady state has been reached, that the dependent variables (velocity, modified pressure and director) have no y dependence, and that the director remains in the xz-plane. These assumptions have been shown to be valid for many common liquid crystals and for moderate flow rates [7]. The velocity $\mathbf{v}$, modified pressure $\tilde{p}$ and director $\mathbf{n}$ can therefore be written as

$$\begin{aligned} &\mathbf{v}=(u(x,z),\,0,\,w(x,z)), \quad \tilde{p}=\tilde{p}(x,z),\\ &\mathbf{n}=(\cos\theta(x,z),\,0,\,\sin\theta(x,z)). \end{aligned} \tag{1}$$

The standard redefinition of pressure p used when studying the Ericksen–Leslie equations has been employed so that the modified pressure $\tilde{p}$ includes a term dependent on orientational elasticity, i.e. $\tilde{p}=p+W$, where $W=W(x,z)$ is the elastic energy per

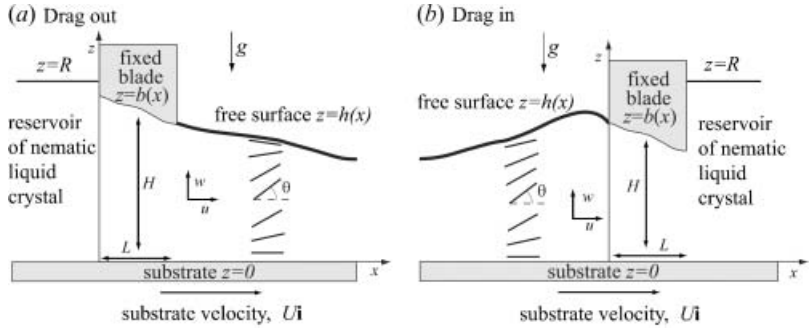

Figure 1. Geometry of the mathematical model for blade coating of a nematic liquid crystal for (*a*) drag out and (*b*) drag in.

unit volume given by

$$2W = K_1(\nabla\cdot\mathbf{n})^2 + K_2(\mathbf{n}\cdot\nabla\times\mathbf{n})^2 + K_3[(\mathbf{n}\cdot\nabla)\mathbf{n}]^2 + (K_2+K_4)\nabla\cdot[(\mathbf{n}\cdot\nabla)\mathbf{n} - (\nabla\cdot\mathbf{n})\mathbf{n}], \quad (2)$$

where K_i for $i=1, 2, 3, 4$ are the elastic constants.

We adopt the following non-dimensionalization:

$$x = Lx^*, \quad z = Hz^*, \quad h = Hh^*,$$
$$b = Hb^*, \quad R = HR^*, \quad \alpha_i = \eta_1\alpha_i^*,$$
$$K_i = K_1K_i^*, \quad u = Uu^*, \quad w = \frac{HU}{L}w^*, \quad (3)$$
$$\tilde{p} - p_a = \frac{\eta_1 UL}{H^2}\tilde{p}^*, \quad Q = UHQ^*,$$

in which we use the typical film thickness $H=(b_0+b_L)/2$, where $b_0=b(0)$ and $b_L=b(L)$ denote the heights of the blade at $x=0$ and $x=L$, respectively; $\eta_1=(\alpha_4+\alpha_3+\alpha_6)/2$, where α_i for $i=1, 2, \ldots, 6$ are the *Leslie viscosities* [6], is one of the *Miesowicz viscosities* [8], p_a is the constant atmospheric pressure, and Q (>0) is the constant volume flux of fluid per unit width, defined by

$$Q = \int_0^h u\,\mathrm{d}z. \quad (4)$$

The standard continuum equations for the behaviour of nematic liquid crystals are the Ericksen–Leslie equations [5–7] which have frequently been shown to model such systems accurately. These equations are nonlinear partial differential equations and consist of a mass conservation equation and balance laws of linear and angular momentum. In order to make analytical progress we will employ certain simplifying assumptions.

Using the standard thin-film approximation [9] based on the assumption that the liquid crystal film is thin, i.e. that H is much smaller than L, so that the aspect ratio ε of the film, defined by $\varepsilon=H/L$, is small, the governing equations can be greatly simplified. This assumption is well justified in many practical coating situations in which a typical liquid crystal film would be of thickness $H=10^{-5}$ m with a typical blade of length $L=10^{-2}$ m or larger, giving $\varepsilon=10^{-3}$ or smaller.

The appropriate thin-film versions of the Ericksen–Leslie equations are

$$0 = \frac{\partial u^*}{\partial x^*} + \frac{\partial w^*}{\partial z^*}, \quad (5)$$

$$0 = \frac{\partial \tilde{p}^*}{\partial x^*} - \frac{\partial}{\partial z^*}\left[g(\theta)\frac{\partial u^*}{\partial z^*}\right] + O(\varepsilon), \quad (6)$$

$$0 = \frac{\partial \tilde{p}^*}{\partial z^*} + G + O(\varepsilon), \quad (7)$$

$$0 = Em(\theta)\frac{\partial u^*}{\partial z^*} - \left[f(\theta)\frac{\partial^2\theta}{\partial z^{*2}} + \frac{1}{2}\frac{\mathrm{d}f(\theta)}{\mathrm{d}\theta}\left(\frac{\partial\theta}{\partial z^*}\right)^2\right] + O(\varepsilon), \quad (8)$$

where

$$g(\theta) = \cos^2\theta + \eta_2^*\sin^2\theta + \alpha_1^*\cos^2\theta\sin^2\theta, \quad (9)$$

$$f(\theta) = \cos^2\theta + K_3^*\sin^2\theta, \quad (10)$$

$$m(\theta) = \alpha_3^*\cos^2\theta - \alpha_2^*\sin^2\theta, \quad (11)$$

in which $\eta_2^*=\eta_2/\eta_1$, where $\eta_2=(\alpha_4+\alpha_5-\alpha_2)/2$ is another of the Miesowicz viscosities [8]. The non-dimensional gravity parameter in equation (7),

$$G = \frac{\rho g H^3}{\eta_1 UL}, \quad (12)$$

is a measure of the relative strength of gravitational and viscous effects, and the non-dimensional *Ericksen number* in equation (8),

$$E = \frac{\eta_1 UH}{K_1}, \quad (13)$$

is a measure of the relative strengths of viscous and elastic effects.

We assume that the free surface is pinned at the downstream end of the blade in the drag-out problem and at the upstream end of the blade in the drag-in problem. At the substrate $z^*=0$ we assume that the director lies parallel to the substrate in the x direction (homogeneous anchoring) and that the fluid velocity is equal to the velocity of the substrate (no slip and no penetration). At the free surface $z^*=h^*(x^*)$ we assume that the usual normal and tangential stress balances hold, and that the director lies parallel to the free surface, as is thought to occur at the free surface of certain nematic liquid crystals. For example, for PAA in the absence of a magnetic field the director lies parallel to the free surface [10–12]. More generally, recent studies show that the orientation at a free surface may depend not only on the particular liquid crystal but also on the speed of the cooling process from the isotropic to the nematic phase [13]. Note that we could alternatively have assumed that the director lies perpendicular to both the substrate and the free surface (homeotropic

anchoring); in that case the following analysis would follow with minor modifications. The appropriately non-dimensionalized boundary conditions are therefore

$$h^* = b_1^* \quad \text{at} \quad x^* = 1 \quad \text{(for drag out)}, \tag{14}$$

$$h^* = b_0^* \quad \text{at} \quad x^* = 0 \quad \text{(for drag in)}, \tag{15}$$

$$\frac{\partial \tilde{p}^*}{\partial x^*} \to 0 \quad \text{as} \quad x^* \to \infty \quad \text{(for drag out)} \quad \text{or} \quad x^* \to -\infty \quad \text{(for drag in)}, \tag{16}$$

$$u^* = 1, \quad w^* = 0, \quad \theta = 0 \quad \text{on} \quad z^* = 0, \tag{17}$$

$$\frac{\partial u^*}{\partial z^*} = 0, \quad \tilde{p}^* = -S\frac{\mathrm{d}^2 h^*}{\mathrm{d}x^{*^2}}, \quad \theta = \varepsilon\frac{\mathrm{d}h^*}{\mathrm{d}x^*} \quad \text{on} \quad z^* = h^*, \tag{18}$$

where $b_0^* = b^*(0)$ and $b_1^* = b^*(1)$ denote the heights of the blade at $x^*=0$ and $x^*=1$, respectively, and the non-dimensional surface-tension parameter in equation (18),

$$S = \frac{\gamma H^3}{\eta_1 U L^3}, \tag{19}$$

is a measure of the relative strength of surface tension and viscous effects. Furthermore, we impose continuity of flux and pressure between the flow under the blade and the flow under the free surface, and continuity of pressure between the flow under the blade and in the reservoir (in which the pressure is assumed to be hydrostatic).

In both the drag-out and drag-in problems the constant flux Q^* is fixed by the conditions far upstream of the blade (i.e. as $x^* \to -\infty$). In the drag-out problem the depth of the reservoir R^* (which can be prescribed *a priori*) determines Q^*. In the drag-in problem the uniform thickness of the film far upstream, which is equal to Q^* (or equivalently in dimensional terms the thickness of the film far upstream, denoted by H_∞, equal to Q/U), can also be prescribed *a priori*.

For a 'flow-aligning' material (i.e. one with $\alpha_2\alpha_3 > 0$ [7]) the flow-alignment angle θ_0, which is defined by $\theta_0 = \tan^{-1}(\alpha_3/\alpha_2)^{\frac{1}{2}}$ and is the angle at which the director would orient to the streamlines in the absence of any elastic or external effects, is usually small. To make analytical progress we restrict our attention to small director angles; in other words, writing θ as $\theta = \delta\theta^*$ with $\theta^* = O(1)$, we assume that $\delta \ll 1$. This is a reasonable assumption because the free surface will be relatively flat (because of the thin-film assumption) and hence the boundary conditions cause only a relatively small director orientation, and the flow induced orientation is small because of the small flow-alignment angle. Hence, at this point we have three small parameters to consider, namely ε, δ and θ_0; the possible orderings of these parameters result in different sets of equations and boundary conditions. In this paper we will discuss two particular orderings, denoted as Cases 1 and 2. The other possible orderings of the small parameters ε, δ and θ_0 are not considered, either because they are not physically realizable, or because they are not tractable analytically (see [4] for further details).

Henceforth we will drop the superscript star from the non-dimensional and scaled variables and consider only non-dimensional and scaled variables unless stated otherwise. In particular, the material constants that appear subsequently are non-dimensionalized according to equation (3) unless stated otherwise.

2.1. Case 1: $\varepsilon \sim \delta \ll \theta_0 \ll 1$

In this case orientational elasticity effects dominate over flow effects which are not sufficiently strong either to achieve flow alignment, or to increase θ significantly from its prescribed value at the boundary. In this case with $\delta = \varepsilon$ the governing equations (5)–(8) simplify to

$$0 = u_x + w_z, \quad 0 = \tilde{p}_x - u_{zz},$$
$$0 = \tilde{p}_z + G, \quad \theta_{zz} = -E_\varepsilon u_z, \tag{20 a-d}$$

where we have introduced the appropriate Ericksen number

$$E_\varepsilon = -\frac{\alpha_3 E}{\varepsilon}. \tag{21}$$

Note that the leading order equations for u and $\tilde{p}$ are independent of θ and that, since $\varepsilon = \delta$, the leading order boundary condition on θ at $z = h$ is $\theta = h_x$.

2.2. Case 2: $\varepsilon \ll \delta \sim \theta_0 \ll 1$

In this case orientational elasticity effects are dominated by flow effects which are sufficiently strong to increase θ significantly from its prescribed value at the boundary and to achieve flow alignment in part of the film. In this case with $\delta = \theta_0$ the governing equations (5)–(8) simplify to

$$0 = u_x + w_z, \quad 0 = \tilde{p}_x - u_{zz},$$
$$0 = \tilde{p}_z + G, \quad \theta_{zz} = -E_{\theta_0}\left(1 - \theta^2\right)u_z \quad , \tag{22 a-d}$$

where we have introduced the appropriate Ericksen number

$$E_{\theta_0} = -\frac{\alpha_3 E}{\theta_0}. \tag{23}$$

Note again that the leading order equations for u and $\tilde{p}$ are independent of θ and that, since $\varepsilon \ll \delta$, the leading order boundary condition on θ at $z=h$ is simply $\theta=0$.

3. Solutions

The leading order equations for the velocity, pressure and director are the same for both the drag-out and the drag-in problems. Moreover, from equations (20 *a–c*) and (22 *a–c*) it is evident that the leading order equations for the fluid velocity and pressure (but not the director) are the same in Cases 1 and 2, and are decoupled from that for the director. Hence for both problems and in both cases we can calculate u, w and $\tilde{p}$ directly from either equations (20 *a–c*) or (22 *a–c*) with boundary conditions (17) and (18) to be

$$u(x, z) = 1 - \frac{\tilde{p}_x}{2}(2h-z)z, \tag{24}$$

$$w(x, z) = \frac{\tilde{p}_{xx}}{6}(3h-z)z^2 + \frac{\tilde{p}_x}{2}h_x z^2, \tag{25}$$

$$\tilde{p}(x, z) = G(h-z) - Sh_{xx}. \tag{26}$$

From equations (4) and (24) we have

$$Q = h - \frac{\tilde{p}_x}{3}h^3, \tag{27}$$

and hence the solution for u may be re-written in the form

$$u = 1 + \frac{3(Q-h)(2h-z)z}{2h^3}, \tag{28}$$

so that the curve $z=z_0$ on which $u=0$ is given by

$$\frac{z_0}{h} = 1 - \left[\frac{3Q-h}{3(Q-h)}\right]^{1/2}. \tag{29}$$

Hence, if $h>3Q$ then there is reverse flow (i.e. $u<0$) when $z_0<z<h$. We can also see from equation (28) that $u_z=0$ not only at the free surface $z=h$, but also when $h=Q$, which will be important in the next two subsections in which we study the director orientation in response to the fluid flow in Cases 1 and 2. Substituting the solution (26) for $\tilde{p}$ into (27) leads to the governing ordinary differential equation for the free surface profile h, namely

$$Sh_{xxx} - Gh_x = \frac{3(Q-h)}{h^3}. \tag{30}$$

In order to impose continuity of pressure between the flow under the blade, the flow under the free surface, and the hydrostatic pressure in the reservoir given by

$$\tilde{p} = G(R-z), \tag{31}$$

we need to know the pressure under the blade. The solution under the blade was analysed in detail in [4], in which it was shown that, under the same approximations as in the present paper, the pressure under the blade is given by the classical Newtonian solution

$$\tilde{p} = \tilde{p}_0 - Gz + 6I_2(x) - 12QI_3(x), \tag{32}$$

where $\tilde{p}_0 = \tilde{p}(0, 0)$ is an undetermined constant and we have introduced the functions $I_n = I_n(x)$ defined by

$$I_n = \int_0^x \frac{1}{b^n(\tilde{x})}\,\mathrm{d}\tilde{x}. \tag{33}$$

In the drag-out problem, imposing continuity of pressure at $x=0$ yields

$$\tilde{p}_0 = GR, \tag{34}$$

and imposing continuity of pressure at $x=1$ yields

$$Sh_{xx}(1) = G(b_1 - R) - 6I_2(1) + 12QI_3(1). \tag{35}$$

Hence, for the drag-out problem the appropriate boundary conditions for equation (30) are (14), (16 *a*) and (35). For a given value of R, this system will have a solution for only one particular value of Q. In practice, it is convenient (and admissible) to replace (35) by

$$h \to Q \quad \text{as} \quad x \to \infty, \tag{36}$$

with Q prescribed *a priori*, and then R can be determined as part of the solution if required.

In the drag-in problem, imposing continuity of pressure at $x=0$ yields

$$\tilde{p}_0 = Gb_0 - Sh_{xx}(0), \tag{37}$$

and imposing continuity of pressure at $x=1$ yields

$$Sh_{xx}(0) = G(b_0 - R) + 6I_2(1) - 12QI_3(1). \tag{38}$$

Hence, for the drag-in problem the appropriate boundary conditions for equation (30) are (15), (16 *b*) and (38), where both R and Q are prescribed *a priori*.

The free surface profile was calculated numerically by solving equation (30) subject to the appropriate boundary

conditions using AUTO [14], a FORTRAN-based software package used to investigate bifurcation problems involving ordinary differential equations. The numerical results will be discussed in detail in the next two sections for the drag-out and the drag-in problem.

We can analyse the asymptotic behaviour of the free surface far downstream in the drag-out problem and far upstream in the drag-in problem. In these two limits we may linearize equation (30) about the uniform solution $h=Q$ by writing $h=Q+\hat{h}$ with $|\hat{h}|\ll 1$ to find that $\hat{h}=\hat{h}(x)$ satisfies

$$S\hat{h}_{xxx}-G\hat{h}_x+\frac{3}{Q^3}\hat{h}=0. \tag{39}$$

In general, the solutions of equation (39) are of the form $\hat{h}=\exp\left[\lambda(G/3S)^{\frac{1}{3}}x\right]$, where λ satisfies

$$\lambda\left(\lambda^2-3\right)+2\sqrt{C}=0, \tag{40}$$

in which the parameter C (>0) is defined by

$$C=\frac{243S}{4G^3Q^6}. \tag{41}$$

The roots of equation (40) determine the nature of the three solutions of (39), monotonic if $\mathrm{Im}(\lambda)=0$, oscillatory if $\mathrm{Im}(\lambda)\neq 0$, and growing or decaying depending on the sign of $\mathrm{Re}(\lambda)$. The number of real and complex roots of (40) depends on the size of C. Specifically, if $C\leqslant 1$ then (40) has one real negative root and two real positive roots, whereas if $C>1$ then (40) has one real negative root and two complex roots with positive real part.

In the limit $x\to\infty$, two of the monotonic solutions of equation (39) for $C\leqslant 1$ and the oscillatory solutions of (39) for $C>1$ are unbounded (and so must be rejected), and hence the appropriate solution of (39) is monotonic, and its decay towards the uniform solution is given by

$$h\sim Q+A_1\exp\left[\lambda_1\left(\frac{G}{3S}\right)^{\frac{1}{3}}x\right], \tag{42}$$

as $x\to\infty$, where A_1 is an undetermined constant and λ_1 is the unique negative real root of (40).

In the limit $x\to-\infty$, if $C\leqslant 1$ then equation (39) has three monotonic solutions, but one of them is unbounded and, of the two bounded solutions, one is dominated by the other, and hence the appropriate solution of (39) is monotonic, and its decay towards the uniform solution is given by

$$h\sim\begin{cases} Q+A_2\exp\left[\lambda_2\left(\dfrac{G}{3S}\right)^{\frac{1}{3}}x\right] & \text{when} \quad C<1,\\ Q+A_2x\exp\left[\lambda_2\left(\dfrac{G}{3S}\right)^{\frac{1}{3}}x\right] & \text{when} \quad C=1, \end{cases} \tag{43}$$

as $x\to-\infty$, where A_2 is an undetermined constant and λ_2 is the smaller of the two positive real roots of (40). On the other hand, if $C>1$ then the monotonic solution of equation (39) is unbounded and hence the appropriate solution of (39) is oscillatory, and its decay towards the uniform solution is given by

$$h\sim Q+\left\{A_3\cos\left[\lambda_4\left(\frac{G}{3S}\right)^{\frac{1}{3}}x\right]+A_4\sin\left[\lambda_4\left(\frac{G}{3S}\right)^{\frac{1}{3}}x\right]\right\}\times\exp\left[\lambda_3\left(\frac{G}{3S}\right)^{\frac{1}{3}}x\right], \tag{44}$$

as $x\to-\infty$, where A_3 and A_4 are undetermined constants and $\lambda_3\pm\mathrm{i}\lambda_4$ are the complex roots of (40) (with positive real part λ_3). In dimensional terms the condition $C>1$ reads

$$\frac{\gamma\eta_1^2U^2}{\rho^3g^3H_\infty^6}>\frac{4}{243}, \tag{45}$$

and hence if the substrate speed U is sufficiently large then the decay of the free surface far upstream of the blade is oscillatory. With typical material parameter values ($\gamma=3.8\times10^{-2}\,\mathrm{N\,m^{-1}}$, $\rho=1168\,\mathrm{kg\,m^{-3}}$, $g=9.8\,\mathrm{m\,s^{-2}}$, $\eta_1=2.4\times10^{-3}\,\mathrm{Pa\,s}$, $K_1=6.9\times10^{-12}\,\mathrm{N}$, $\alpha_2=-6.9\times10^{-3}\,\mathrm{Pa\,s}$, $\alpha_3=-2\times10^{-4}\,\mathrm{Pa\,s}$ [7]) and $H_\infty=10^{-5}\,\mathrm{m}$ the condition (45) gives $U>U_{c1}$, where $U_{c1}\simeq3.4\times10^{-7}\,\mathrm{m\,s^{-1}}$, meaning that (since a typical substrate speed in a standard blade-coating process is $U=0.05$–$1\,\mathrm{m\,s^{-1}}$ [3]) in practice the decay far upstream will be oscillatory.

3.1. Case 1: $\varepsilon\sim\delta\ll\theta_0\ll1$

In this case orientational elasticity effects dominate over flow effects and we expect the flow to have only a weak effect on the director. Substituting the solution (28) for u into the angular momentum balance (20 d), integrating twice and applying boundary conditions (17) and (18) leads to the solution for θ, namely

$$\theta=\frac{h_x}{h}z+E_e\frac{(Q-h)(h-z)(2h-z)z}{2h^3}. \tag{46}$$

The solution (46) shows that the flow changes the director profile from a linear profile due to purely elastic effects when $E_e=0$ to a cubic profile when $E_e\neq0$, and that as flow effects become more important (i.e. as the Ericksen number increases) the director is distorted further away from the linear profile.

3.2. Case 2: $\varepsilon\ll\delta\sim\theta_0\ll1$

In this case the angular momentum balance (22 d) must, in general, be solved numerically for θ. However, when

the Ericksen number is large, i.e. when $E_{\theta_0} \gg 1$, flow effects dominate over orientational elasticity effects and the solution for θ in the bulk is simply $\theta = 1$ (equivalent to the unscaled flow-alignment angle θ_0) when $u_z > 0$ and $\theta = -1$ (equivalent to the unscaled flow-alignment angle $-\theta_0$) when $u_z < 0$, with two thin orientational boundary layers within which θ changes rapidly to its prescribed boundary values, one near the substrate $z = 0$ and the other near the free surface $z = h$. The solution for the director within these thin orientational boundary layers is found by applying standard boundary-layer analysis [15] and following the approach used in our previous work [4].

To analyse the orientational boundary layer near the substrate $z = 0$, which is of thickness d_0 ($\ll h$), where

$$d_0 = \frac{h}{(3|h-Q|E_{\theta_0})^{1/2}}, \tag{47}$$

we introduce the inner variables Z and $\Theta = \Theta(Z)$ defined by

$$Z = \frac{z}{d_0}, \quad \Theta(Z) = \mathrm{sgn}(h-Q)\theta(x, z). \tag{48}$$

At leading order Θ satisfies

$$\Theta_{ZZ} = 1 - \Theta^2, \tag{49}$$

subject to $\Theta(0) = 0$ and $\Theta \to -1$ as $Z \to \infty$, with the appropriate solution

$$\Theta = 2 - 3\tanh^2\left(\frac{Z}{\sqrt{2}} + \tanh^{-1}\sqrt{\frac{2}{3}}\right). \tag{50}$$

Similarly, to analyse the orientational boundary layer near the free surface $z = h$, which is of thickness d_h ($\ll h$), where

$$d_h = \frac{h}{(3|h-Q|E_{\theta_0})^{1/3}}, \tag{51}$$

we introduce the inner variables ζ and $\phi = \phi(\zeta)$ defined by

$$\zeta = \frac{h-z}{d_h}, \quad \phi(\zeta) = \mathrm{sgn}(h-Q)\theta(x, z). \tag{52}$$

At leading order ϕ satisfies

$$\phi_{\zeta\zeta} = \zeta(1-\phi^2) \tag{53}$$

subject to $\phi(0) = 0$ and $\phi \to -1$ as $\zeta \to \infty$. In [4] a trivially re-scaled version of equation (53) was solved numerically to yield a monotonically decreasing solution for ϕ.

An appropriate composite uniformly valid leading-order asymptotic solution for θ is therefore

$$\theta \sim \mathrm{sgn}(h-Q)\left\{3\ \mathrm{sech}^2\left[\left(\frac{3|h-Q|E_{\theta_0}}{2}\right)^{1/2}\frac{z}{h} + \beta\right] + \phi\left((3|h-Q|E_{\theta_0})^{1/3}\frac{h-z}{h}\right)\right\}, \tag{54}$$

where $\beta = \tanh^{-1}\sqrt{2/3}$.

In equation (50), and thereby (54), a choice of signs has been made to rule out higher energy solutions; details of a similar choice are given in [4].

Note that, since $E_{\theta_0} \gg 1$, both orientational boundary layers are thin provided that h is not too close to Q, and hence the present boundary-layer analysis fails both near any value of x at which $h = Q$ and as $|x| \to \infty$. In particular, if $h = Q$ at $x = x_0$, say, then the boundary layers grow to fill the film when $|x - x_0| = O(E_{\theta_0}^{-1})$, while, since $h \sim Q$ according to equation (42) as $x \to \infty$ for drag out and according to (43) or (44) as $x \to -\infty$ for drag in, the boundary layers always grow to fill the film when $|x| = O(\log E_{\theta_0})$. A detailed analysis of the regions near $x = x_0$ is an interesting topic for further work.

In the next two sections we present specific details of the velocity and the director in the drag-out and the drag-in problems.

4. Drag-out problem

In this section we consider the drag-out problem, in which the substrate $z = 0$ moves away from the fixed blade, see figure 1 (*a*). We calculate the free surface profile numerically by solving equation (30) subject to the boundary conditions (14), (16*a*) and (36). In this case we find that there is a unique solution. Furthermore, we find that if $Q < b_1$ ($Q > b_1$) then the free surface profile decreases (increases) monotonically from its prescribed value $h = b_1$ at $x = 1$ to $h = Q < b_1$ ($h = Q > b_1$) as $x \to \infty$.

Figure 2 shows the velocity vectors in the particular case of a uniform blade $b \equiv 1$, when $S = G = 1$ and $Q = 0.25$. In this case there is a region of reverse flow above the curve $z = z_0$ on which $u = 0$ (indicated with a full line) when $h > 3Q = 0.75$.

The director in Case 1, given by equation (46), is shown in figure 3 in the particular case of a uniform blade $b \equiv 1$, when $S = G = 1$ and $Q = 0.25$ for (a) $E_\varepsilon = 1$ and (b) $E_\varepsilon = 10$. In general, for values of E_ε lying in the interval $0 < E_\varepsilon < E_{\varepsilon c}$, where the critical value $E_{\varepsilon c}$ is given by

$$E_{\varepsilon c} = \min_{x>1}\left(\frac{2h_x}{Q-h}\right), \tag{55}$$

so that in this case $E_{\varepsilon c} \simeq 6.48$, the director profile is

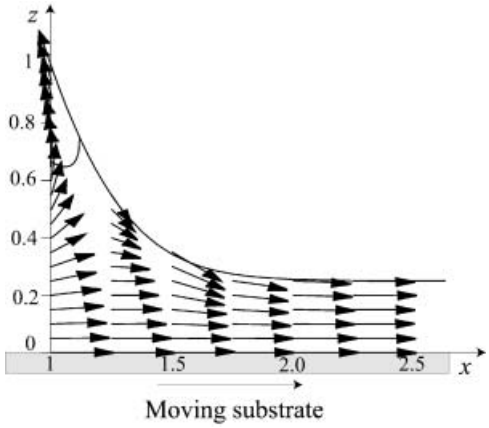

Figure 2. The velocity vectors in the drag-out problem when $b\equiv1$, $S=G=1$ and $Q=0.25$. Reverse flow occurs above the curve $z=z_0$ on which $u=0$ (indicated with a full line) when $h>3Q=0.75$.

monotonic, see figure 3 (*a*) whereas for values of E_ε satisfying $E_\varepsilon > E_{\varepsilon c}$ the flow causes the director to develop a minimum if $Q<b_1$, see figure 3 (*b*), or a maximum if $Q>b_1$ (not shown for brevity) within the film.

The director in Case 2, given by equation (54), is shown in figure 4 in the particular case of a uniform blade $b\equiv1$, when $S=G=1$ and $Q=0.25$ for $E_{\theta_0}=10^4$, and clearly shows the orientational boundary layers near the substrate and the free surface. Note that in the drag-out problem the shear never changes sign; thus $\theta=-1$ ($\theta=1$) everywhere in the bulk if $Q<b_1$ ($Q>b_1$).

5. Drag-in problem

In this section we consider the drag-in problem, in which the substrate $z=0$ moves towards the fixed blade, see figure 1 (*b*). The free surface again satisfies equation (30), which must now be solved subject to the boundary conditions (15), (16*b*) and (38). In this case we find that there may be multiple (steady) solutions depending on the relative sizes of S, G and Q. In figure 5 we present a typical GQ-parameter plane showing the number of solutions in the different regions when $S=1$ in the particular case of a uniform blade $b\equiv1$ and a reservoir of depth $R=2$. In particular, figure 5 shows that when $G=0$ there is a unique solution for values of Q lying in the interval $0<Q<Q_{c1}(0)$, where $Q_{c1}(0)\simeq0.500$, there are two solutions for values of Q lying in the interval $Q_{c1}(0)<Q<Q_{c2}(0)$, where $Q_{c2}(0)\simeq0.651$, and there is no solution for values of Q satisfying $Q>Q_{c2}(0)$. As figure 5 also shows, when $G\neq0$ there are two possibilities. On one hand, if $0<G<G_c$, where $G_c\simeq0.215$, then there are either one or three solutions, depending on the value of Q; specifically, there is a unique solution for values of Q lying in the interval $0<Q<Q_{c1}(G)$, there are three solutions for values of Q lying in the interval $Q_{c1}(G)<Q<Q_{c2}(G)$, and there is again a unique solution for values of Q satisfying $Q>Q_{c2}(G)$. On the other hand, if $G>G_c$ then there is a unique solution for all values of Q. Note that, as figure 5 shows, $Q_{c1}(G_c)=Q_{c2}(G_c)\simeq0.647$.

In order to determine which of these solutions might occur in practice we would need to study their energy and/or stability to small perturbations. This analysis is not pursued here but is the subject of ongoing work and will be discussed in a subsequent publication; however it might be expected on physical grounds that when three solutions occur, two of them are stable.

In figures 6, 7 and 8 we show the velocity vectors and the director in Cases 1 and 2, respectively, in the particular case of a uniform blade $b\equiv1$ and a reservoir of depth $R=2$, when $S=1$, $G=0.2$ and $Q=0.64$, parameter values for which there are three solutions and the decay of the free surface far from the blade is oscillatory. Specifically, figure 6 shows that there is a region of reverse flow above the curve $z=z_0$ on which $u=0$ [indicated with a full line in figures 6 (*b*) and 6 (*c*)]

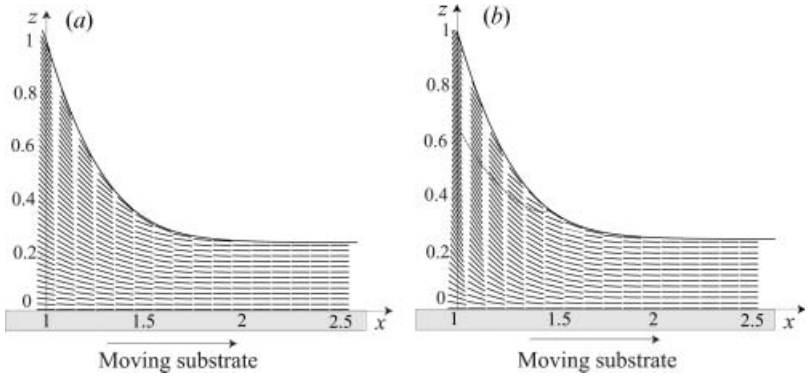

Figure 3. The director in the drag-out problem in Case 1 when $b\equiv1$, $S=G=1$ and $Q=0.25$ for (*a*) $E_\varepsilon=1$ and (*b*) $E_\varepsilon=10$. The curve on which $\theta_z=0$ is indicated with a dashed line (for a minimum).

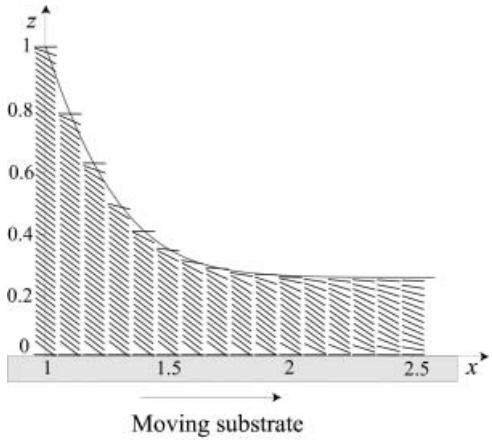

Figure 4. The director in the drag-out problem in Case 2 when $b\equiv1$, $S=G=1$ and $Q=0.25$ for $E_{\theta_0}=10^4$.

when $h>3Q=1.92$. Furthermore, there is a change in the sign of the shear when h passes through Q. Figure 7 shows the director in Case 1 for $E_\varepsilon=5$ whose profile develops a zero, a maximum (indicated with a full line), and a minimum (indicated with a dashed line) within the film. Figure 8 shows the director in Case 2 for $E_{\theta_0}=10^4$; in particular, it shows the orientational boundary layers near the substrate and the free surface. Figure 8 also shows how the director changes its orientation in the bulk from $\theta=+1$ to $\theta=-1$ according to the sign of the shear.

Figure 9 shows the director in Case 1 in the particular case of a uniform blade $b\equiv1$ and a reservoir of depth $R=2$, when $S=1$, $G=10$ and $Q=0.7$ for $E_\varepsilon=5$, parameter values for which there is a unique solution and the decay of the free surface far from the blade is monotonic. In this case the director profile develops a zero and a minimum (indicated with a dashed line) within the film. For these parameter values the director in Case 2 (not shown for brevity) is similar to that

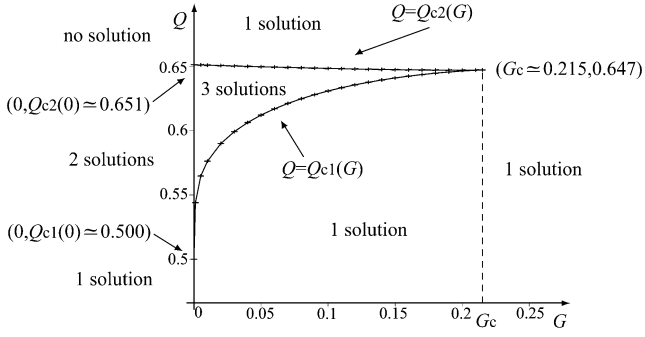

Figure 5. GQ-parameter plane showing the number of solutions in the different regions when $b\equiv1$, $R=2$ and $S=1$. The crosses indicate numerically calculated points on the boundary curves $Q=Q_{c1}(G)$ and $Q=Q_{c2}(G)$.

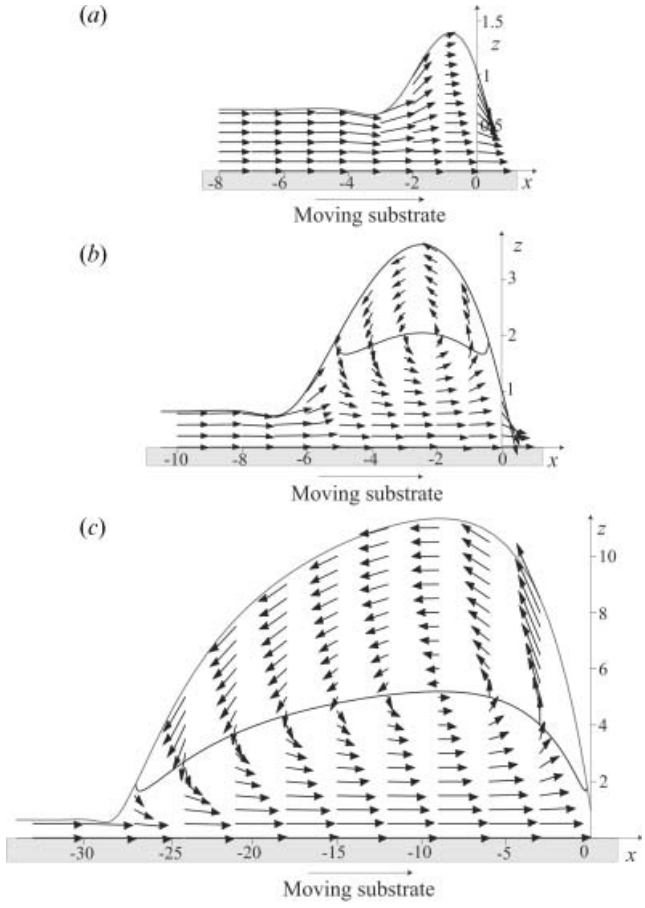

Figure 6. The velocity vectors in the drag-in problem when $b\equiv1$, $R=2$, $S=1$, $G=0.1$ and $Q=0.64$, parameter values for which there are three solutions and the decay of the free surface far from the blade is oscillatory. Reverse flow occurs above the curve $z=z_0$ on which $u=0$ [indicated with a full line in (*b*) and (*c*)] when $h>3Q=1.92$.

shown in figure 8 (*c*) with $\theta=-1$ in the bulk and orientational boundary layers near the substrate and the free surface.

6. Conclusions

Using the Ericksen–Leslie equations we have analysed the flow and alignment of a thin film of a nematic liquid crystal during a blade-coating process, both after emerging from the region under a blade (drag out) and before entering the region under a blade (drag in). Analytical and numerical progress was made in the case when the liquid crystal film is thin and the director angle is small. In particular, analytical solutions for the fluid velocity and pressure and the director in Case 1 were found; the solution for the director in Case 2 requires the numerical solution of a parameter-free system.

In the drag-out problem we found that there is a unique solution and that the decay of the free surface

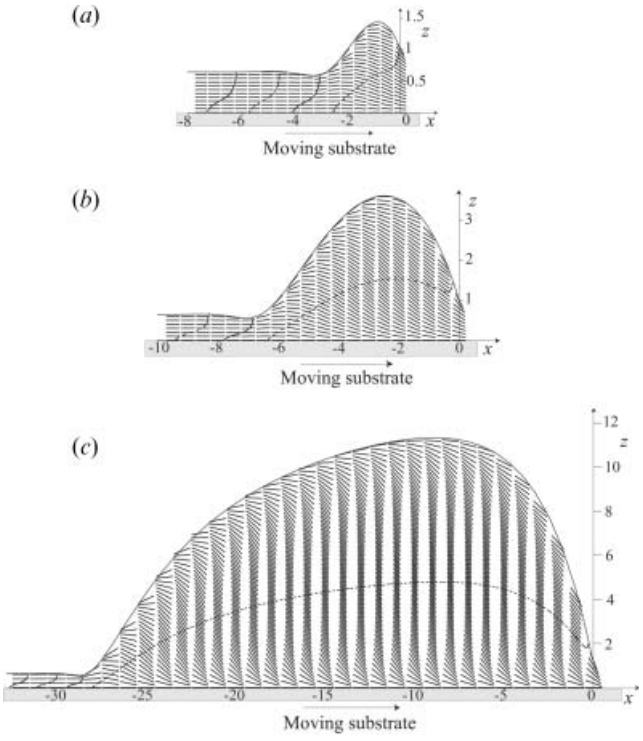

Figure 7. The director in the drag-in problem in Case 1 when $b\equiv1$, $R=2$, $S=1$, $G=0.1$ and $Q=0.64$ for $E_\varepsilon=5$, parameter values for which there are three solutions and the decay of the free surface far from the blade is oscillatory. The curve on which $\theta_z=0$ is indicated with a full line (for a maximum) or a dashed line (for a minimum).

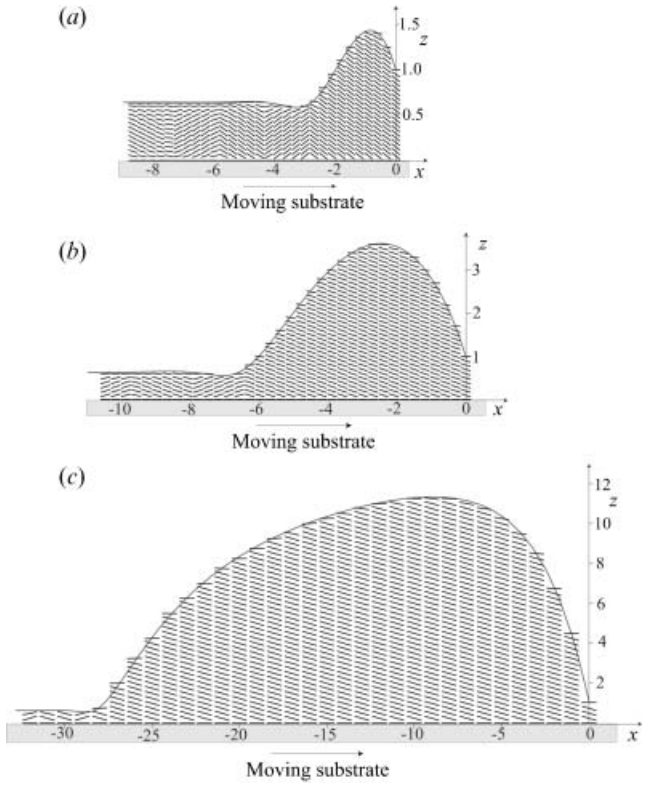

Figure 8. The director in the drag-in problem in Case 2 when $b\equiv1$, $R=2$, $S=1$, $G=0.1$ and $Q=0.64$ for $E_{\theta_0}=10^4$, parameter values for which there are three solutions and the decay of the free surface far from the blade is oscillatory.

towards its uniform solution far from the blade is monotonic; furthermore, numerical results suggested that the free surface is monotonic for all x. When elastic effects dominate, the director is monotonic for values of E_ε smaller than the critical value $E_{\varepsilon c}$ given by equation (55), and otherwise the director develops a minimum (if $Q<b_1$) or a maximum (if $Q>b_1$) within the film. When flow effects dominate, the director aligns at an angle $-\theta_0$ (if $Q<b_1$) or θ_0 (if $Q>b_1$) in the bulk, with thin orientational boundary layers near the substrate and the free surface.

In the drag-in problem we found that there may be one, two or three solutions and that the decay of the free surface towards its uniform solution far from the blade can be either monotonic or oscillatory depending on the relative sizes of S, G and Q. In particular, as figure 5 shows, when $b\equiv1$, $R=2$ and $S=1$ there is a unique solution for all values of Q when $G>G_c\simeq0.215$, and a unique solution for all values of G when $Q>Q_{c2}(0)\simeq0.651$. With typical material parameter values, $H=10^{-5}$ m and $L=(\gamma/\eta_1 U)^{1/3}H$ the conditions $G>G_c$ and $Q>Q_{c2}(0)$ give $U<U_{c2}$ and $H_\infty>H_{\infty c}$, respectively, where $U_{c2}\simeq2.6\times10^{-5}\,\mathrm{m\,s^{-1}}$ and $H_{\infty c}\simeq6.5\times10^{-6}$ m, meaning that multiple solutions could well occur in practice. When elastic effects dominate, the film always contains regions where the director is non-monotonic. When flow effects dominate, the director changes its orientation from $-\theta_0$ to θ_0 (or *vice*

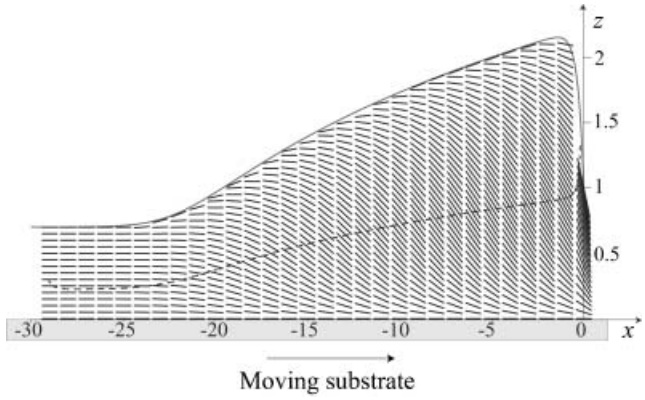

Figure 9. The director in the drag-in problem in Case 1 when $b\equiv1$, $R=2$, $S=1$, $G=10$ and $Q=0.7$ for $E_\varepsilon=5$, parameter values for which there is a unique solution and the decay of the free surface far from the blade is monotonic. The curve on which $\theta_z=0$ is indicated with a dashed line (for a minimum).

versa) in the bulk when $h=Q$, with thin orientational boundary layers near the substrate and the free surface.

In both the drag-in and drag-out problems it may in practice be desirable to minimize the distortion of the director as much as possible to ensure a homogeneous orientation of the liquid crystal. Where large distortions of the director occur it may be possible for defects in the orientation to nucleate. This would be particularly likely to occur close to the substrate where any imperfection or impurity in the substrate may trigger such a nucleation process if the director is highly distorted. From the present results we see that there is significant director distortion within the liquid crystal film in Case 1 when the Ericksen number E_ε is relatively large. This distortion could be avoided in the drag-out problem by keeping E_ε smaller than $E_{\varepsilon c}$. Typically E_ε is large, meaning that this distortion is likely to occur in practice. However, since this distortion appears within the film and not near the substrate, the likelihood of defect nucleation may not be as high as it might appear. Of more importance is the relatively large director distortion that appears close to the substrate in Case 2 when E_{θ_0} is large. Typically E_{θ_0} is large, meaning that this distortion is also likely to occur in practice. In the drag-out problem (in which the shear never changes sign) this distortion could be avoided if the pretilt director value at the substrate is taken to be $-\theta_0$ (if $Q<b_1$) or θ_0 (if $Q>b_1$), and thus the risk of the appearance of defects minimized. However, if this pretilt value is difficult to achieve in real applications, then the relatively slow speeds needed to avoid large gradients in the director mean that they are likely to occur in practice. The regions near to where $h=Q$, in which the boundary layers grow to fill the film, could also be potential locations for the nucleation of defects. All of these findings suggest that coating in the isotropic phase is preferable to coating in the nematic phase. However, for optical elements where a high degree of ordering is needed it may be preferable to utilize the increase in order parameter due to flow alignment. This possibility suggests that the situation in Case 2 may provide an advantage if the orientational order is 'frozen in' soon after the fluid emerges from under the blade.

Finally, we note that throughout this paper we assumed that $\alpha_2<0$ (as it is for calamitic liquid crystals) and $\alpha_3<0$, so that the material is flow-aligning, i.e. $\theta_0=\tan^{-1}(\alpha_3/\alpha_2)^{\frac{1}{2}}$ is defined. If $\alpha_2<0$ and $\alpha_3>0$ then the liquid crystal is non-flow-aligning, i.e. θ_0 is not defined; in such a case, if the director remains in the plane of shear, the present analysis follows through with only minor differences. Furthermore, the present analysis is also relevant to *discotic* liquid crystals (i.e. liquid crystals whose constituent molecules are disc-like rather than rod-like) for which $\alpha_3>0$ [16]. A more detailed discussion of the relevance of the present analysis to non-flow-aligning calamitics and flow-aligning and non-flow-aligning discotics can be found in [4].

Acknowledgements

J.Q.C. wishes to thank the University of Strathclyde for financial support via a Graduate Teaching Assistantship, and N.J.M. wishes to thank EPSRC for financial support via an Advanced Research Fellowship.

References

[1] G.P. Crawford. *Flexible Flat Panel Displays*. Wiley, Chichester (2005).
[2] R. Penterman, S.I. Klink, H. de Koning, G. Nisato, D.J. Broer. *Nature*, **417**, 55 (2002).
[3] S.F. Kistler, P.M. Schweizer. *Liquid Film Coating*. Chapman & Hall, London (1997).
[4] J. Quintans Carou, B.R. Duffy, N.J. Mottram, S.K. Wilson. *Phys. Fluids*, **18**, 027105-1 (2006).
[5] J.L. Ericksen. *Arch. Ration. Mech. Anal.*, **4**, 231 (1960).
[6] F.M. Leslie. *Q. J. Mech. appl. Math.*, **19**, 357 (1966).
[7] I.W. Stewart. *The Static and Dynamic Continuum Theory of Liquid Crystals*. Taylor & Francis, London (2004).
[8] M. Miesowicz. *Nature*, **158**, 27 (1946).
[9] H. Ockendon, J.R. Ockendon. *Viscous Flow*. Cambridge University Press, Cambridge (1995).
[10] V. Naggiar. *C. R. Acad. Sci.*, **208**, 1916 (1939).
[11] M.A. Bouchiat, D. Langevin-Cruchon. *Phys. Lett.*, **34A**, 331 (1971).
[12] B. Jerome. *Rep. Prog. Phys.*, **54**, 391 (1991).
[13] V. Nazarenko, A. Nych. *Phys. Rev. E*, **60**, R3495 (1999).
[14] E. Doedel. *Cong. Numer.*, **30**, 265 (1981).
[15] A.H. Nayfeh. *Perturbation Methods*. Wiley, New York (1973).
[16] S. Chandrasekhar. In *Handbook of Liquid Crystals, Vol. 2B* edited by, D. Demus, J. Goodby, G.W. Gray, H.-W. Spiess, V. Vill (Eds), pp. 749–780, Wiley-VCH, Weinheim (1998).